

Non-contact Non-destructive Evaluation via Air-coupled Focused Ultrasound and Laser Vibrometry

Haoyu Fu, Yanfeng Shen*

University of Michigan-Shanghai Jiao Tong University Joint Institute, Shanghai Jiao Tong University, Shanghai, 200240, China

ABSTRACT

Air-coupled ultrasonic NDE techniques avoid the procedure of installing transducers and the unwanted characteristics brought by the coupling material. Problems such as limited diagnostic resolution, low energy penetration and poor acoustic coupling greatly limit the application of this promising technique. This paper presents a novel non-contact NDE system, combining focused air-coupled ultrasound and a single-point laser Doppler vibrometer. A focal piezoelectric transducer along with its backing layer, which is capable of focusing air-coupled ultrasound and collaborating with the vibrometer, is designed, numerically studied, and manufactured. The resonant motion of the transducer is settled by a backing layer, and the ultrasonic focusing effectively overcomes the problem of low resolution and weak penetration. A 6D robotic arm is programmed to mobilize the focal transmitter and the vibrometer, so as to control the orientation and location of the non-contact transmission and reception. The scanning function carried out by the robotic arm and the high precision provided by the vibrometer further increase the resolution of the non-contact NDE system. An algorithm is developed through analyzing the received signal at each scanning points for realizing the damage imaging, in which the signal energy is utilized to derive a damage index. Through experiments on a composite specimen, the system's strong capability for damage evaluation is verified. The paper finishes with concluding remarks and suggestions for future work.

Keywords: non-contact NDE; air-coupled ultrasonics; laser vibrometry; damage imaging

1. INTRODUCTION

Ultrasonic non-destructive evaluation (NDE) plays a pivotal role in ensuring the structural integrity of high-end aerospace and mechanical components [1, 2]. Ultrasonic NDE techniques have proven efficacious due to significant advantages such as high sensitivity and simplicity [3-6]. These attributes make ultrasonic techniques particularly important as NDE techniques for complex structures [6-8]. Consequently, much research has been dedicated to the development of effective methodologies for generating and propagating ultrasonic waves within structures [9-11].

Immersion ultrasonic inspection, requiring immersing the inspected component in water, is considered a method for ultrasonic NDT [12, 13]. However, the existence of liquid may do harm to composite structures, while at the same time reducing the feasibility of the methods [14]. A similar situation applies to usage of other liquid acoustic couplants [15, 16]. In recent years, the most common way to excite ultrasonics involves coupling transducers directly to the surface of the structure applying adhesives or other bonding materials [17]. This method helps retain the maximum amount of acoustic energy while minimizing the effects of acoustic impedance mismatch between the transducers and the target structures, thus improving the performance of the ultrasound system [18-20]. On the other hand, the installation of arrays of transducers over large areas can be time-consuming and labor-intensive. Moreover, the presence of the transducers themselves can introduce unwanted interference or noise, which may complicate the analysis and affect the accuracy of the results [21].

In order to avoid these problems brought by the contact between specimen and coupling material, laser ultrasonics, which applies lasers and optical methods to generate and detect ultrasonic waves, is proposed and developed [22, 23]. Still, problems that the high-energy laser which is responsible for generating ultrasonic waves may do harm to the specimen surface, undermine the feasibility of the technique [24]. In contrast, air-coupled ultrasonic techniques offer a promising alternative by eliminating the need for direct contact between the transducers and the structure [25-28]. This method simplifies the setup and avoids the unpredictable characteristics associated with coupling agents [29, 30]. However, air-coupled ultrasonic NDE faces significant challenges such as poor acoustic coupling, limited diagnostic resolution, and insufficient energy penetration [31-33]. These limitations have made it difficult to fully leverage the potential of air-coupled ultrasonic technology in practical inspections. As a result, there is a growing demand for innovative solutions that can overcome these obstacles and unlock the full potential of air-coupled ultrasonic NDE [32, 34, 35]. Addressing these

challenges could significantly enhance the versatility and efficiency of air-coupled ultrasonic NDE, making it a more viable tool for non-contact, large-scale inspections.

This paper proposes a novel approach to conducting non-contact NDE, combining focused ultrasound emitted by a focal piezoelectric transducer (FPT) and a miniature laser Doppler vibrometer for mechanical wave measurements. Therefore, compared with conventional air-coupled ultrasound technique, this method renders a small, focused area of aucton, achieving high spatial resolution, while the laser Doppler vibrometry directly pick up the surface particle motion, facilitating strong and reliable measurement signal. This research starts with a numerical study on the characteristics and performance of the FPT. After that, the FPT is manufactured and combined with the laser Doppler vibrometer utilizing customized fixtures. Finally, a 6D robotic arm is programed to mobilize the transmission-reception pair. A LabVIEW User Interface (UI) is designed to define the scanning function. The effectiveness of the system is demonstrated by damage imaging experiments of a composite panel with impact damage.

2. NUMERICAL INVESTIGATION ON THE AIR-COUPLED ULTRASONIC FOCAL PIEZOELECTRIC TRANSDUCER

In order to achieve greater intensity and higher spatial resolution of the air-coupled ultrasonic excitation, a piezoelectric focal transducer (FPT) was proposed and studied numerically. The acoustic wave focusing effect will be demonstrated. The importance of a gradient-property backing layer will be highlighted to settle ringing effects which could complex the interrogative wavefield.

2.1 FE model configurations

The 2D symmetric script and the corresponding 3D model for simulating the transducer's behavior were constructed in COMSOL, as shown in Figure 1. The FPT responsible for emitting air-coupled ultrasound is a dome-shaped piezoelectric (PZT-5H) wafer, polarized along the thickness direction, with the upper surface functioning as the grounding electrode, and the lower surface serving as the positive electrode. The focal polarization can be achieved through a transformation of coordinate system:

$$\begin{aligned} x_1 &= \sin(\arctan \frac{y}{x})x - \cos(\arctan \frac{y}{x})y \\ x_2 &= \cos(\arctan \frac{y}{x})x + \sin(\arctan \frac{y}{x})y \end{aligned} \quad (1)$$

where x and y denote Cartesian coordinate system; x_1 and x_2 denote the transformed coordinate system. A hole with 3.6 mm in diameter is manufactured at the center of the transducer to let pass the laser beam. The focal radius is set to be 50 mm, the diameter of the orthographic projection of the transducer spans 50 mm, and the thickness is 2.5 mm. On top of the piezoelectric components, five layers of damping material, with a thickness of 2 mm for each layer, is implemented, functioning as the backing layer for absorbing the reflected ultrasonic waves caused by the acoustic impedance mismatch between the transducer and air. The numerical settings of the density and elasticity matrix of the backing material ensure a smooth transition of acoustic impedance from the transducer to air.

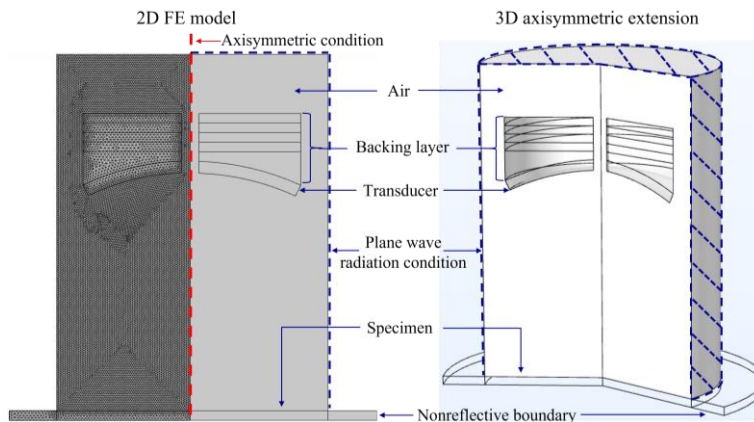


Figure 1. The 2D model and corresponding 3D axisymmetric extension for finite element analysis.

In the simulation model, air surrounds the transducer, with plane wave radiation set at the boundaries to dissipate the acoustic waves. At the bottom of the model, a 2-mm thickness aluminum plate is placed, so that the focal point of the transducer falls on the upper surface of the plate. Non-reflective boundaries are applied on the plate to avoid reflection of wave energy. Unstructured triangular mesh is generated for the model, with the largest mesh size stipulated to be smaller than one-twentieth the size of the smallest wavelength under consideration, so as to ensure the accuracy of the simulation results.

2.2 Investigation on the focusing behavior

The effect of the focusing behavior of the FPT was investigated first using numerical simulations. A planar air-coupled transmitter with exactly the same parameters and settings was deployed for comparison. The backing layer was removed from both focal and planar transducers to exclude other interference. It is worth mentioning that due to the limited sampling frequency of the laser Doppler vibrometer used later in this study, the excitation frequency for the transducer mainly ranges within the best working spectrum from 1 kHz to 500 kHz. An excitation amplitude of 100 V_{pp} was used for both transducers. The vibration responses in vertical direction of the aluminum plate at the focal point were extracted for comparison, as shown in Figure 2.

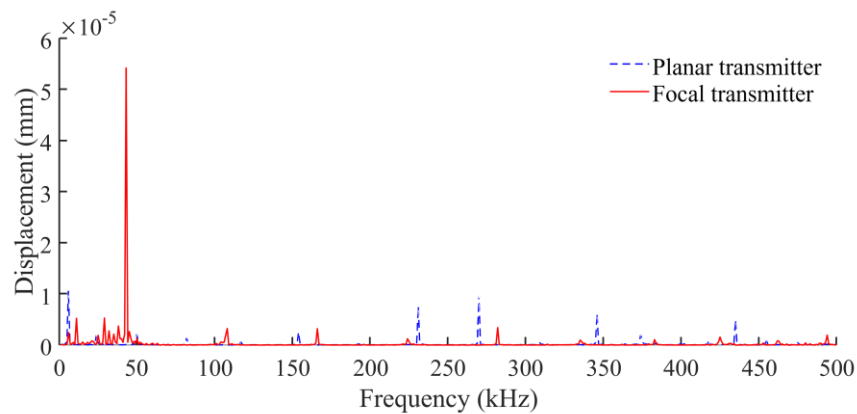


Figure 2. Frequency tuning results for planar (blue dashed line) and focal (red solid line) transmitters in FE analysis.

These results verify that under the excitation at a sweet frequency, the FPT is capable of emitting ultrasonic waves into the specimen with much higher amplitude compared with the ordinary planar air-coupled transducer with the same size and material. The sweet frequency, 43 kHz in this case, was chosen and used for further numerical analysis.

2.3 Investigation on the effectiveness of the backing layer

Due to the high acoustic impedance mismatch between the transducer material and air, wave energy will be reflected back and forth between the transducer front and back surfaces as the transducer is emitting air-coupled ultrasonic signals, resulting in a ringing effect. In order to achieve high resolution in temporal domain, the elimination of such a ringing effect is needed. A backing layer was developed to absorb the backward propagating waves, acting as a non-reflective boundary for the transducer, to avoid multiple reflections of waves in the transducer. Transient analyses were conducted for the transducer without and with the backing layer to verify the effectiveness of the backing material. The excitation signal is a 1.5-count tone burst with a center frequency of 43 kHz and an excitation amplitude of 100 V.

The ultrasonic pressure fields generated by the transducers were compared, as shown in Figure 3(a, b). It was found that for the transducer without the backing layer, the vibration barely stopped, and the ultrasonic wave signal was continuously emitted from the transducer into the air, towards the specimen. While for the one attached with the backing layer, only one major ultrasonic wave packet was observed in the air, indicating the effectiveness of the backing layer. Also, it was observed that most acoustic energy was concentrated in a relatively small area along the center line of the model, indicating that the FPT is capable of generating air-coupled ultrasonic signal with good spatial resolution.

Comparing the displacement in vertical direction of the specimen at the focal point in two cases, presented in Figure 3(c, d), it is clear that the transducer with the backing layer leads to far cleaner burst-type response signal, further proving the effectiveness and necessity of the backing layer.

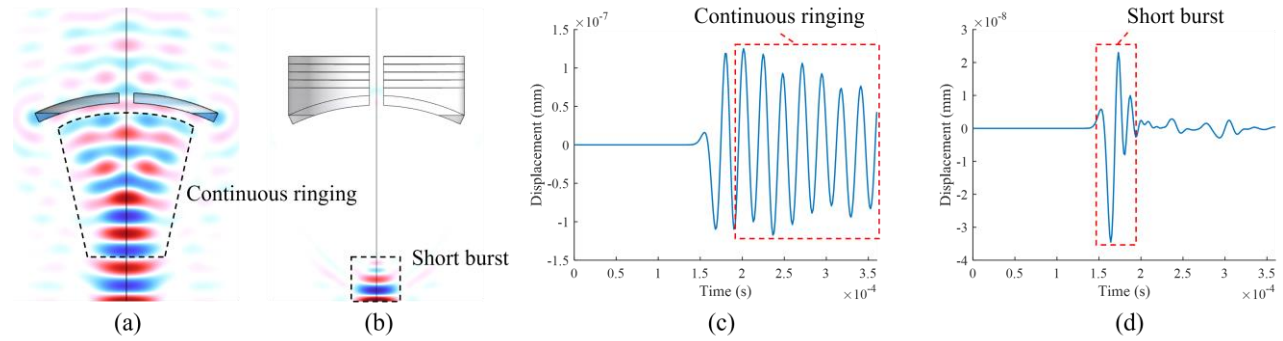


Figure 3. Ultrasonic acoustic wavefield generated by the transducers in FE analysis: (a) transducer without backing layers; (b) transducer attached with backing layers; out-of-plane displacement of the target specimen excited by (c) transducer without backing layers; (d) transducer attached with backing layers.

2.4 Investigation on the effectiveness of FPT in evaluating different kinds of damage

Finally, samples with various types of damage were used in the simulation to verify the feasibility of the FPT. The types of damage include a tenfold reduction in Young’s modulus, material loss on the upper surface, and material loss on the lower surface. Through analyzing the vertical displacement response at the focal point, as shown in Figure 4, significant variation of signal amplitude can be observed, indicating that the intensity of specimen’s vibration response at the focal point of the FPT can be used for damage detection.

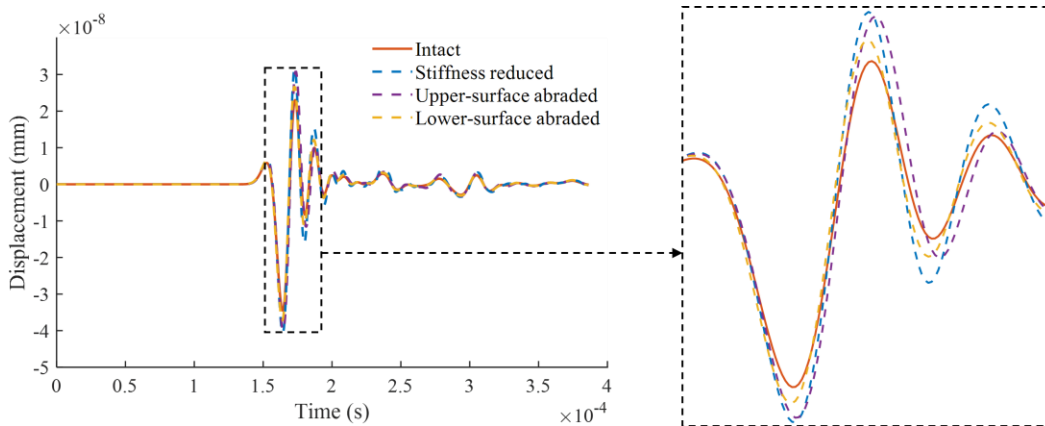


Figure 4. Out-of-plane displacement of the target specimen with different statuses: intact (orange solid line), stiffness reduced (blue dashed line), upper-surface abraded (purple dashed line), and lower-surface abraded (yellow dashed line).

3. DESIGN, MANUFACTURING, AND CONSTRUCTION OF THE NDE SYSTEM

In order to build a non-contact NDE system with high resolution and accuracy. The FPT along with the backing layer was manufactured to function as the air-coupled ultrasonic transmitter. For the reception of the signal, a single-point laser Doppler vibrometer is applied to obtain the vibration information. Besides, a 6D robotic arm is deployed to carry the transducers so as to fulfill the scanning function.

3.1 Design and manufacturing of the FPT

The piezoelectric material used for fabricating the FPT is P-81, of which the main chemical composition is zirconium oxide, titanium oxide, and lead oxide. The ingredients were mixed, pre-fired and dry pressed with the customized mold. Then the green body was put in the high-temperature furnace and turned into dense ceramics. After that, conductive layers were formed on the upper and lower surfaces of the ceramic by printing electrodes. Finally, the ceramic was polarized by exerting an external electric field on the electrodes. Figure 5(a) presents the focal piezoelectric plate fabricated.

After the fabrication of the piezoelectric component, layers of backing materials were implemented on the back surface of the transducer. The composition of the material mainly consists of high-damping resin and ceramic powder. The resin is

to damp out the reflected energy, while the role of the ceramic powder is to match the acoustic impedance so as to reduce reflection. The ceramic powder content in the backing material increases with proximity to the piezoelectric component in a gradient fashion, so as to provide a smooth transition of the acoustic impedance among layers of backing materials. Figure 5(b) demonstrates the resin mixed with ceramic powder of different mass fraction.

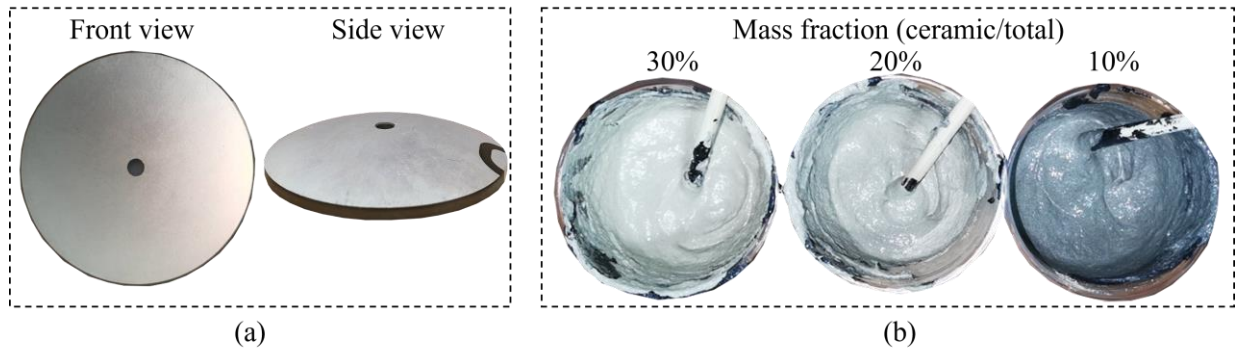


Figure 5. (a) Focal piezoelectric component (front and side views); (b) backing materials containing ceramic of different mass fraction (30%, 20%, and 10%).

The effectiveness of the backing layer produced was verified through analyzing the vibration response of the surface of the transducer under excitation. The excitation signal was a 1.5-count Hanning window modulated sine tone burst. A laser Doppler vibrometer was used to obtain the transducer's out-of-plane velocity, and the results are shown in Figure 6. It was observed that the transducer attached with the backing layer quickly ceased vibration after excitation, whereas the transducer without the backing layer continued to vibrate for a much longer period due to multiple reflections of wave energy as a ringing effect.

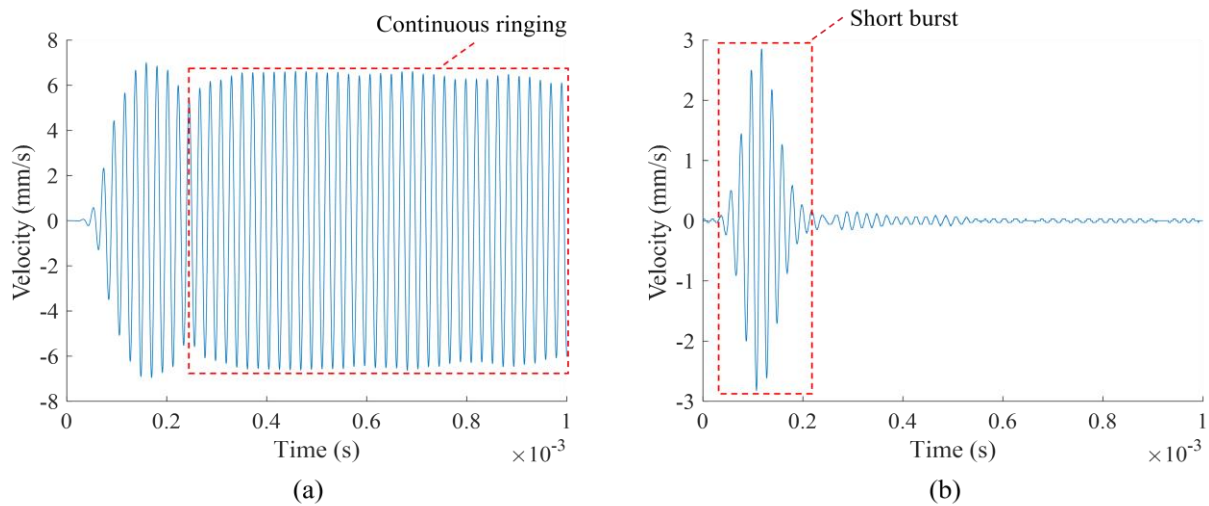


Figure 6. The out-of-plane velocity of the transducer (a) without the backing layers; (b) attached with the backing layers.

3.2 Design and construction of the non-contact NDE system

The main experimental apparatus of the NDE system includes an NI PXIe-1071 waveform generator, an Aigtek ATA-4014 power amplifier, an OSP MotionGo single-point laser Doppler vibrometer, a LEBAI 6D robotic arm, and the FPT. A custom-designed fixture structure not only connects and secures the vibrometer and the FPT along with the robotic arm, but also makes sure that the laser beam shoots through the hole of the FPT and aims at the focal point of the transducer. Figure 7 presents the composition of the FPT, the function of the fixture, and the relative position between the FPT and the vibrometer.

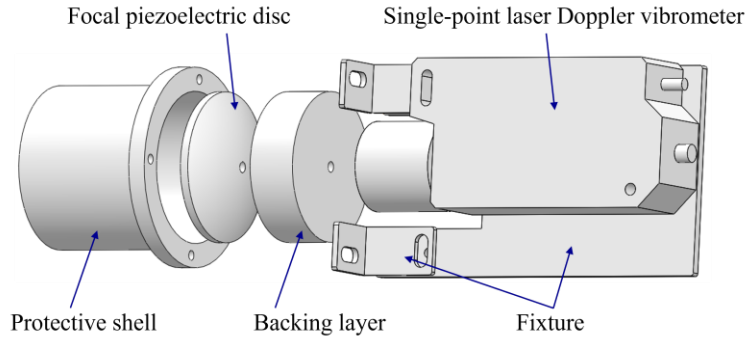


Figure 7. Exploded view of the combined transducer system.

The goal of the NDE system is to conduct an air-coupled ultrasonic excitation and laser vibration measurement for each single point in the defined scanning area on the specimen. The workflow of the system is presented in Figure 8. When the system begins to work, the NI LabView system first sends the posture adjustment order to the robotic arm. The robotic arm then carries the transducer to the desired location which is programmed in advance. After that, the NI control board sends the excitation signal to the power amplifier and the amplified signal is delivered to the FPT, driving the FPT to generate focused ultrasound. As the focused ultrasound arrives at the specimen, it will penetrate the target structure and cause dynamic response in the vicinity of the focal point. Then, the out-of-plane vibration response on the specimen is collected by the laser Doppler vibrometer and delivered back to the NI control board for further data postprocessing. This is the complete roadmap for the inspection at one single point. After these procedures, the NI control board starts a new loop and the robotic arm travels to a new spot for evaluation.

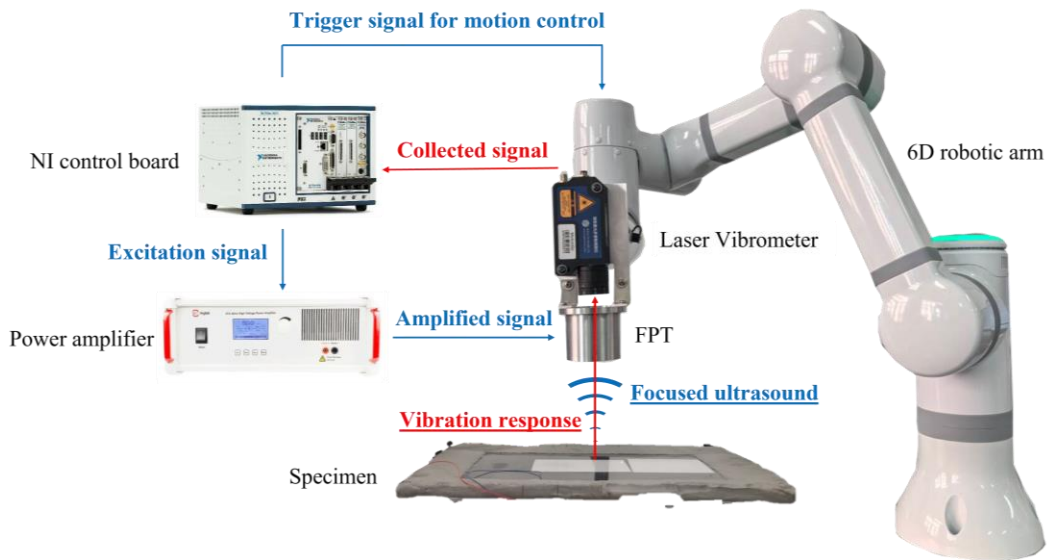


Figure 8. Experimental setup and workflow of the non-contact NDE system.

4. EXPERIMENTAL VERIFICATION OF THE NDE SYSTEM

To verify the performance of the system, a carbon fiber reinforced polymer (CFRP) plate with an impact damage was used as the target specimen for inspecting. After conducting a frequency tuning test, the excitation frequency for the FPT was set to be 51 kHz, and the excitation waveform was a 1.5-count Hanning window modulated sine tone burst signal. The scanning resolution of the 6D robotic arm was set to be 1 mm, and a scanning area of 100 mm* 160 mm was defined for the specimen. The signal excitation and vibration measurements were conducted 15 times at each scanning point, and the average value was calculated to eliminate noise. According to the discussion made in the FE analysis, the intensity of the collected signal was used to characterize the status of the specimen. A damage index (DI) was derived to indicate the damage condition at each scanning point, the formula is

$$DI = \{ \max_{t \in [t_1, t_2]} \sqrt{[(x * h)(t)]^2 + \mathcal{H}[(x * h)(t)]^2} - \mu \} / \sigma \quad (2)$$

where $x(t)$ is the out-of-plane displacement collected at the scanning point, t_1 and t_2 specify the time domain for the first wave packet of the received signal, μ and σ are the corresponding average value and standard deviation of the maximum values, $h(t)$ represents the impulse response of the filter, which can be represented as

$$h(t) = 2f_2 \cdot \text{sinc}(2f_2 t) - 2f_1 \cdot \text{sinc}(2f_1 t) \quad (3)$$

where f_1 and f_2 are the lower frequency limit and the upper frequency limit, correspondingly. \mathcal{H} is the Hilbert transform function, which can be written as

$$\mathcal{H}\{x(t)\} = \frac{1}{\pi} \text{p.v.} \int_{-\infty}^{\infty} \frac{x(\tau)}{t - \tau} d\tau \quad (4)$$

The proposed damage index represents the signal intensity after conducting bandpass filtering and extracting the envelope of the raw signal. The values are then normalized for improving imaging quality. As long as sites of damage exist, the local stiffness of the material shall be affected, leading to a dramatic change in the energy of the specimen's response. The signal intensity was utilized as the indicator for the response energy.

The picture of the specimen and the imaging result are shown in Figure 9(a, b). Due to the impact damage on the CFRP plate, the local stiffness was reduced, leading to a higher displacement response under the air-coupled ultrasonic excitation. The damage imaging result verifies that the system is able to assess the damage location, thus demonstrating the performance of the system.

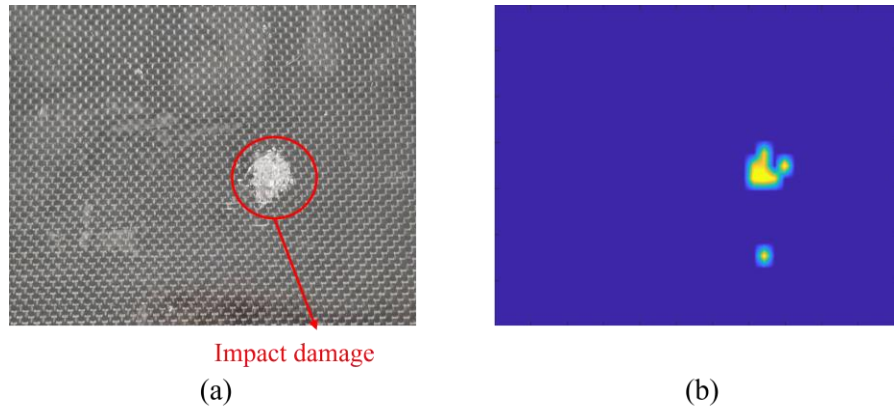


Figure 9. (a) Picture of the CFRP plate with the impact damage; (b) Damage imaging result for the CFRP plate with the impact damage.

5. CONCLUDING REMARKS AND SUGGESTIONS FOR FUTURE WORK

This paper propounded a novel approach to conducting non-contact NDE, combining focused ultrasound emitted by a focal piezoelectric transducer (FPT) and laser Doppler vibrometer for mechanical wave measurements. The FPT responsible for transmitting air-coupled ultrasound effectively overcame the problem of traditional air-coupled methods' low resolution and weak penetration, as it greatly increased the ultrasonic energy sent into the specimen. The fabricated backing layer played an important role in settling the resonance of the transducer. A laser Doppler vibrometer was employed for picking up wave response in the specimen, achieving a complete non-contact NDE test setup. The orientation and location of the transmission and reception components were controlled via a 6D robotic arm, fulfilling the scanning function. A signal processing algorithm was developed through analyzing the received signal at each scan point for realizing the damage imaging. Finally, the composite specimen with an impact damage was examined by the proposed non-contact NDE system. The results demonstrated the system's strong capability for damage evaluation.

Future work will focus on further development of the FPT with piezoelectric fibers, deeper understanding of the ultrasonic focusing effect, and optimization on the system design to improve the scanning speed.

ACKNOWLEDGEMENTS

The support from the National Natural Science Foundation of China (contract number 52475161) is thankfully acknowledged. Dr. Yanfeng Shen appreciates the funding from John Wu & Jane Sun Endowed Professorship.

REFERENCES

- [1] G. D. Prete *et al.*, "Laser Ultrasonic Non-Destructive Testing for Aerospace Applications," in *2023 IEEE 10th International Workshop on Metrology for AeroSpace (MetroAeroSpace)*, 19-21 June 2023 2023, pp. 525-528, doi: 10.1109/MetroAeroSpace57412.2023.10189937.
- [2] Z. Shao *et al.*, "A Review of Non-Destructive Evaluation (NDE) Techniques for Residual Stress Profiling of Metallic Components in Aircraft Engines," *Aerospace*, vol. 9, no. 10, doi: 10.3390/aerospace9100534.
- [3] C. J. Lissenden, "Nonlinear ultrasonic guided waves—Principles for nondestructive evaluation," *Journal of Applied Physics*, vol. 129, no. 2, p. 021101, 2021, doi: 10.1063/5.0038340.
- [4] Z. Ma *et al.*, "Nondestructive Evaluation of Stress Corrosion Cracking in a Welded Steel Plate Using Guided Ultrasonic Waves," *Journal of Nondestructive Evaluation, Diagnostics and Prognostics of Engineering Systems*, vol. 5, no. 3, 2022, doi: 10.1115/1.4053653.
- [5] J. Wang, M. Schmitz, L. J. Jacobs, and J. Qu, "Deep learning-assisted locating and sizing of a coating delamination using ultrasonic guided waves," *Ultrasonics*, vol. 141, p. 107351, 2024/07/01/ 2024, doi: <https://doi.org/10.1016/j.ultras.2024.107351>.
- [6] J. C. Aldrin, J. S. Knopp, E. A. Lindgren, and K. V. Jata, "MODEL-ASSISTED PROBABILITY OF DETECTION EVALUATION FOR EDDY CURRENT INSPECTION OF FASTENER SITES," *AIP Conference Proceedings*, vol. 1096, no. 1, pp. 1784-1791, 2009, doi: 10.1063/1.3114175.
- [7] J. C. Aldrin *et al.*, "Investigations of pitch-catch angled-beam ultrasonic NDE for characterization of hidden regions of impact damage in composites," *AIP Conference Proceedings*, vol. 2102, no. 1, p. 040012, 2019, doi: 10.1063/1.5099762.
- [8] A. Mardanshahi, M. M. Shokrieh, and S. Kazemirad, "Identification of matrix cracking in cross-ply laminated composites using Lamb wave propagation," *Composite Structures*, vol. 235, p. 111790, 2020/03/01/ 2020, doi: <https://doi.org/10.1016/j.compstruct.2019.111790>.
- [9] J. Chang, Z. Chu, X. Gao, A. I. Soldatov, and S. Dong, "A magnetoelectric-ultrasonic multimodal system for synchronous NDE of surface and internal defects in metal," *Mechanical Systems and Signal Processing*, vol. 183, p. 109667, 2023/01/15/ 2023, doi: <https://doi.org/10.1016/j.ymsp.2022.109667>.
- [10] A. Ramos, A. Ruiz, and E. Riera, "Modeling Pulsed High-Power Spikes in Tunable HV Capacitive Drivers of Piezoelectric Wideband Transducers to Improve Dynamic Range and SNR for Ultrasonic Imaging and NDE," *Sensors*, vol. 21, no. 21, doi: 10.3390/s21217178.
- [11] K. Zou, Q. Yue, J. Li, W. Zhang, R. Liang, and Z. Zhou, "High-performance ultrasonic transducer based on PZT piezoelectric ceramic for high-temperature NDE," *Ultrasonics*, vol. 132, p. 107013, 2023/07/01/ 2023, doi: <https://doi.org/10.1016/j.ultras.2023.107013>.
- [12] R. Raišutis, R. Kažys, and L. Mažeika, "Application of the ultrasonic pulse-echo technique for quality control of the multi-layered plastic materials," *NDT & E International*, vol. 41, no. 4, pp. 300-311, 2008.
- [13] S. A. Titov, R. G. Maev, and A. N. Bogachenkov, "Pulse-echo NDT of adhesively bonded joints in automotive assemblies," *Ultrasonics*, vol. 48, no. 6-7, pp. 537-546, 2008.
- [14] B. Ehrhart, B. Valeske, C.-E. Muller, and C. Bockenheimer, "Methods for the quality assessment of adhesive bonded CFRP structures—a resumé," in *2nd International Symposium on NDT in Aerospace*, 2010, vol. 2010.
- [15] C. Li and E. Nordlund, "Effects of couplants on acoustic transmission," *Rock mechanics and rock engineering*, vol. 26, no. 1, pp. 63-69, 1993.
- [16] M. A. Stuber Geesey, B. Aristorenas, T. J. Ulrich, and C. M. Donahue, "Investigation of the nonlinearity of transducer acoustic couplants for nonlinear elastic measurements," *NDT & E International*, vol. 104, pp. 10-18, 2019/06/01/ 2019, doi: <https://doi.org/10.1016/j.ndteint.2019.03.004>.
- [17] D. A. Derusova, V. P. Vavilov, V. O. Nekhoroshev, V. Y. Shpil'noi, and N. V. Druzhinin, "Features of Laser-Vibrometric Nondestructive Testing of Polymer Composite Materials Using Air-Coupled Ultrasonic Transducers," *Russian Journal of Nondestructive Testing*, vol. 57, no. 12, pp. 1060-1071, 2021/12/01 2021, doi: 10.1134/S1061830921120044.

- [18] K. Balasubramaniam, S. Sikdar, P. Fiborek, and P. H. Malinowski, "Ultrasonic Guided Wave Signal Based Nondestructive Testing of a Bonded Composite Structure Using Piezoelectric Transducers," *Signals*, vol. 2, no. 1, pp. 13-24doi: 10.3390/signals2010002.
- [19] A. Hadizade, S. H. Kamali, and M. Moallem, "A Time-Domain Method for Ultrasound Concrete Health Monitoring Using In Situ Piezoelectric Transducers," *IEEE Transactions on Instrumentation and Measurement*, vol. 72, pp. 1-9, 2023, doi: 10.1109/TIM.2023.3238033.
- [20] J. Yin, Z. Zhou, and L. Lou, "A Novel Nondestructive Testing Probe Using AlN-Based Piezoelectric Micromachined Ultrasonic Transducers (PMUTs)," *Micromachines*, vol. 15, no. 3, doi: 10.3390/mi15030306.
- [21] J. Nagpal, R. Rana, R. Lal, R. Muttanna Singari, and H. Kumar, "A brief review on various effects of surface texturing using lasers on the tool inserts," *Materials Today: Proceedings*, vol. 56, pp. 3803-3812, 2022/01/01/ 2022, doi: <https://doi.org/10.1016/j.matpr.2022.01.272>.
- [22] A. Zarei and S. Pilla, "Laser ultrasonics for nondestructive testing of composite materials and structures: A review," *Ultrasonics*, vol. 136, p. 107163, 2024/01/01/ 2024, doi: <https://doi.org/10.1016/j.ultras.2023.107163>.
- [23] S. K. DATTA, "Ultrasonic and electromagnetic NDE for structure and material characterization engineering and biomedical applications," ed: Acoustical Society of America, 2013.
- [24] A. D. Abetew, T. C. Truong, S. C. Hong, J. R. Lee, and J. B. Ihn, "Parametric optimization of pulse-echo laser ultrasonic system for inspection of thick polymer matrix composites," *Structural Health Monitoring*, vol. 19, no. 2, pp. 443-453, 2020/03/01 2020, doi: 10.1177/1475921719852891.
- [25] Y. Bernhardt and M. Kreutzbruck, "Integrated defect sensor for the inspection of fiber-reinforced plastics using air-coupled ultrasound," *J. Sens. Sens. Syst.*, vol. 9, no. 1, pp. 127-132, 2020, doi: 10.5194/jsss-9-127-2020.
- [26] H. Selim, R. Picó, J. Trull, M. D. Prieto, and C. Cojocar, "Directional Ultrasound Source for Solid Materials Inspection: Diffraction Management in a Metallic Phononic Crystal," *Sensors*, vol. 20, no. 21, doi: 10.3390/s20216148.
- [27] J. Hinrichs, M. Sachsenweger, M. Rutsch, G. Allevato, W. M. D. Wright, and M. Kupnik, "Lamb waves excited by an air-coupled ultrasonic phased array for non-contact, non-destructive detection of discontinuities in sheet materials," in *2021 IEEE International Ultrasonics Symposium (IUS)*, 11-16 Sept. 2021 2021, pp. 1-4, doi: 10.1109/IUS52206.2021.9593363.
- [28] J. Hinrichs, C. Haugwitz, M. Rutsch, G. Allevato, J. H. Dörsam, and M. Kupnik, "Simulation of Lamb Waves Excited by an Air-Coupled Ultrasonic Phased Array for Non-Destructive Testing," in *2022 IEEE International Ultrasonics Symposium (IUS)*, 10-13 Oct. 2022 2022, pp. 1-4, doi: 10.1109/IUS54386.2022.9957266.
- [29] E. Ahn, M. Shin, and J. S. Popovics, "Air-coupled ultrasonic diffuse-wave techniques to evaluate distributed cracking damage in concrete," *Ultrasonics*, vol. 125, p. 106800, 2022/09/01/ 2022, doi: <https://doi.org/10.1016/j.ultras.2022.106800>.
- [30] B. Wang *et al.*, "Non-contact detection of the interfacial microdefects in metal/CFRP hybrid composites using air-coupled laser ultrasound," *Structural Health Monitoring*, vol. 24, no. 1, pp. 243-254, 2025/01/01 2024, doi: 10.1177/14759217241234557.
- [31] J. Zhou, J. Bai, and Y. Liu, "Fabrication and Modeling of Matching System for Air-Coupled Transducer," *Micromachines*, vol. 13, no. 5, doi: 10.3390/mi13050781.
- [32] M. Boccaccio, P. Rachiglia, G. P. Malfense Fierro, G. Pio Pucillo, and M. Meo, "Deep-Subwavelength-Optimized Holey-Structured Metamaterial Lens for Nonlinear Air-Coupled Ultrasonic Imaging," *Sensors*, vol. 21, no. 4, doi: 10.3390/s21041170.
- [33] C.-M. Kang *et al.*, "Acoustic and rheological characterization of hollow glass microsphere composite for development of optimized air-coupled ultrasonic matching layer," *Ceramics International*, vol. 48, no. 21, pp. 32036-32048, 2022/11/01/ 2022, doi: <https://doi.org/10.1016/j.ceramint.2022.07.141>.
- [34] X. Wenfeng and Y. Lingyu, "Non-contact passive sensing of acoustic emission signal using the air-coupled transducer," in *Proc.SPIE*, 2021, vol. 11593, p. 1159327, doi: 10.1117/12.2583218. [Online]. Available: <https://doi.org/10.1117/12.2583218>
- [35] L. Yu, W. Xiao, H. Mei, and V. Giurgiutiu, "Delamination imaging in composites using cross-correlation method by non-contact air-coupled Lamb waves," *Smart Materials and Structures*, vol. 32, no. 10, p. 105013, 2023/09/06 2023, doi: 10.1088/1361-665X/acf178.